MICROTUBULE ORGANIZATION 1 Regulates Structure and Function of Microtubule Arrays during Mitosis and Cytokinesis in the Arabidopsis Root[1][W]

Eiko Kawamura, Regina Himmelspach[2], Madeleine C. Rashbrooke, Angela T. Whittington[3], Kevin R. Gale[3], David A. Collings, and Geoffrey O. Wasteneys*

Department of Botany, University of British Columbia, Vancouver, British Columbia, Canada V6T 1Z4 (E.K., G.O.W.); Plant Cell Biology Group, Research School of Biological Sciences, Australian National University, Canberra, Australian Capital Territory 2601, Australia (E.K., R.H., M.C.R., A.T.W., D.A.C., G.O.W.); and Commonwealth Scientific and Industrial Research Organization, Plant Industry, Canberra, Australian Capital Territory 2601, Australia (K.R.G.)

MICROTUBULE ORGANIZATION 1 (MOR1) is a plant member of the highly conserved MAP215/Dis1 family of microtubule-associated proteins. Prior studies with the temperature-sensitive *mor1* mutants of Arabidopsis (*Arabidopsis thaliana*), which harbor single amino acid substitutions in an N-terminal HEAT repeat, proved that MOR1 regulates cortical microtubule organization and function. Here we demonstrate by use of live cell imaging and immunolabeling that the *mor1-1* mutation generates specific defects in the microtubule arrays of dividing vegetative cells. Unlike the universal cortical microtubule disorganization in elongating *mor1-1* cells, disruption of mitotic and cytokinetic microtubule arrays was not detected in all dividing cells. Nevertheless, quantitative analysis identified distinct defects in preprophase bands (PPBs), spindles, and phragmoplasts. In nearly one-half of dividing cells at the restrictive temperature of 30°C, PPBs were not detected prior to spindle formation, and those that did form were often disrupted. *mor1-1* spindles and phragmoplasts were short and abnormally organized and persisted for longer times than in wild-type cells. The reduced length of these arrays predicts that the component microtubule lengths are also reduced, suggesting that microtubule length is a critical determinant of spindle and phragmoplast structure, orientation, and function. Microtubule organizational defects led to aberrant chromosomal arrangements, misaligned or incomplete cell plates, and multinucleate cells. Antiserum raised against an N-terminal MOR1 sequence labeled the full length of microtubules in interphase arrays, PPBs, spindles, and phragmoplasts. Continued immunolabeling of the disorganized and short microtubules of *mor1-1* at the restrictive temperature demonstrated that the mutant mor1-1^{L174F} protein loses function without dissociating from microtubules, providing important insight into the mechanism by which MOR1 may regulate microtubule length.

Microtubules are an essential feature of eukaryotic cells as they divide, change shape, and transport organelles. Microtubule-associated proteins (MAPs) play crucial roles in organizing microtubules. MICROTUBULE ORGANIZATION 1 (MOR1) of Arabidopsis (*Arabidopsis thaliana*) belongs to the MAP215/Dis1 family of MAPs (Whittington et al., 2001), a highly conserved group of MAPs found in all eukaryotes examined to date (Gard et al., 2004). MOR1 was initially discovered through the isolation of two mutants that both undergo temperature-dependent cortical microtubule disorganization, which leads to the left-handed twisting and eventual radial swelling of organs. Both mutations substitute single amino acids (*mor1-1*^{L174F} and *mor1-2*^{E195K}) in an N-terminal HEAT repeat, one of many such motifs found extensively along the length of MOR1 and other MAP215/Dis1 family proteins (Whittington et al., 2001). Another *mor1* allele, *rid5*, has a similar morphological phenotype to the *mor1* mutants. The *rid5* mutation has a single amino acid substitution near the N terminus and was identified in a screen for a temperature-sensitive impairment of auxin-dependent adventitious root formation (Konishi and Sugiyama, 2003). *MOR1* occurs as a single-copy gene in Arabidopsis (Whittington et al., 2001) and severe alleles are considered to be homozygous-lethal (Twell et al., 2002). Understanding the function of MOR1 therefore relies on the identification of weak alleles or ones that generate severe defects only under specific

[1] This work was supported by the Australian Research Council (DP0208872), the Natural Sciences and Engineering Research Council of Canada (298264–04), and Bayer CropScience. E.K. received an Australian National University Ph.D. Scholarship and a University of British Columbia Graduate Fellowship.

[2] Present address: Office of the Gene Technology Regulator, Pharmacy Guild House, 15 National Circuit, Barton, ACT 2600, Australia.

[3] Present address: Policy Coordination and Environment Protection Division, Department of the Environment and Heritage, GPO Box 787, Canberra, ACT 2601, Australia.

* Corresponding author; e-mail geoffwas@interchange.ubc.ca; fax 604–822–6089.

The author responsible for distribution of materials integral to the findings presented in this article in accordance with the policy described in the Instructions for Authors (www.plantphysiol.org) is: Geoffrey O. Wasteneys (geoffwas@interchange.ubc.ca).

[W] The online version of this article contains Web-only data.

Article, publication date, and citation information can be found at www.plantphysiol.org/cgi/doi/10.1104/pp.105.069989.

conditions. The temperature-sensitive *mor1-1*, *mor1-2*, and *rid5* alleles are clearly valuable tools for understanding the function of the wild-type protein.

In the initial study of *mor1* mutants, obvious defects in cortical microtubule arrays of interphase and terminally differentiating cells developed rapidly at 29°C, but mitotic and cytokinetic microtubule arrays did not show obvious defects and cell division continued (Whittington et al., 2001). Tissue patterns and cell numbers in the root elongation zone were the same in *mor1-1* and wild type, suggesting that the enlarged diameter of the *mor1-1* root tip was generated entirely by radial expansion and not through addition of extra cell layers. Furthermore, the effects of treatment at the restrictive temperature for several weeks were reversible, suggesting that apical meristems were well preserved (Whittington et al., 2001). These results were puzzling, given that all MOR1 homologs previously identified in animal and fungal cells have been shown to be essential for spindle formation and function (Gard et al., 2004).

The likely function of MOR1 in cell division was first supported by the finding that *MOR1* gene expression peaks during the M phase of Arabidopsis suspension culture cells (Menges et al., 2002) and the discovery that the *gemini1* mutants, which affect cell plate formation in haploid microspores, were allelic to *MOR1* (Twell et al., 2002). Twell et al. (2002) did not investigate whether microtubules were disrupted in *gem1* microspores, but they did report immunological evidence for partial colocalization of MOR1 protein and microtubules in preprophase bands (PPBs), spindles, and phragmoplasts of Arabidopsis suspension culture cells. Using an antiserum raised against a C-terminal fragment of expression protein, they described a concentration of antibody at the midline of phragmoplasts and posited that MOR1/GEM1 stabilizes microtubule plus ends at the zone of microtubule overlap. More recently, the tobacco (*Nicotiana tabacum*) homolog of MOR1, MAP200, which was originally purified from tobacco BY-2 cells in telophase (Yasuhara et al., 2002), has also been immunolocalized in the vicinity of microtubule arrays during cell division (Hamada et al., 2004).

The apparent lack of obvious division defects in the temperature-sensitive *mor1* mutants after short treatments at 29°C (Whittington et al., 2001) prompted us to consider the possibility that the specific amino acid substitutions near the N terminus may be inconsequential for microtubule function during cell division. On closer examination, however, we noted that *mor1-1* root tips swell more severely above the threshold restrictive temperature of 29°C and after prolonged (on the order of 24–48 h) incubations. After root tips of *mor1-1* were treated at 30°C for 48 h, we observed incomplete cross walls and other indications of aberrant cell division (Himmelspach et al., 2003a). Recently, these observations have been confirmed (Eleftheriou et al., 2005).

Here we investigate the subcellular distribution and function of the MOR1 protein in dividing cells of the mutant *mor1-1* root tip, using restrictive temperatures at or above 30°C, which rapidly induce microtubule disruption and promote root radial swelling. Using live cell imaging and immunolabeling approaches we show that, in addition to the anticipated defects in phragmoplast arrays, MOR1 is also clearly important for the structure and function of PPBs and spindles. We observed many cells entering mitosis without first forming PPBs and observed heavily disrupted spindles, which correlated with significant delays in the progression of cell division. In contrast to the findings of Twell et al. (2002), we demonstrate that the MOR1 protein colocalizes along the entire length of microtubules at all stages of the cell cycle and that, in the *mor1-1* mutant, a single amino acid substitution in the N terminus leads to microtubule disorganization at restrictive temperatures without abolishing binding to microtubules.

RESULTS

Aberrant Cell Wall Formation and Multinucleate Cells in *mor1-1* Root Tips

Preliminary examination by transmission electron microscopy of *mor1-1* root-tip cells treated at 31°C for 48 h revealed incomplete cell walls, wall stubs, and, occasionally, internal wall fragments or inclusions (data not shown). To confirm that these aberrant formations were part of the cell wall, we labeled transverse and longitudinal sections of root tips with an antibody specific for xyloglucan, the principal hemicellulosic component of Arabidopsis cell walls. Fluorescence microscopy revealed xyloglucan distribution to the incomplete and aberrant cell wall formations (Fig. 1, A–D). Multinucleate cells, another indicator of aberrant cytokinesis, were commonly observed in *mor1-1* (Fig. 1, E and F). We confirmed by optical sectioning that as many as four or five nuclei were clustered together in single *mor1-1* cells (Fig. 1F). These findings clearly indicated to us that cell division is affected in the *mor1-1* mutants.

Mitosis and Cytokinesis Are Retarded in *mor1-1* Mutants at the Restrictive Temperature

To examine whether the *mor1-1* mutation affects the frequency of cell division, we compared the proportion of cells undergoing mitosis in wild-type and *mor1-1* root tips that were fixed and stained after 24 h at 31°C (Fig. 2). We detected a significant (*t* test, $P < 0.05$) increase in the mitotic index in *mor1-1* for both the cortex and endodermis, and a slight but statistically nonsignificant ($P < 0.15$) increase in the epidermis. These findings indicate that either mitosis proceeds more slowly in *mor1-1* or that the cell production rate is increased relative to wild type.

To compare the duration of mitosis and cytokinesis in *mor1-1* and wild type, we examined microtubules in living root tips of plants stably transformed to

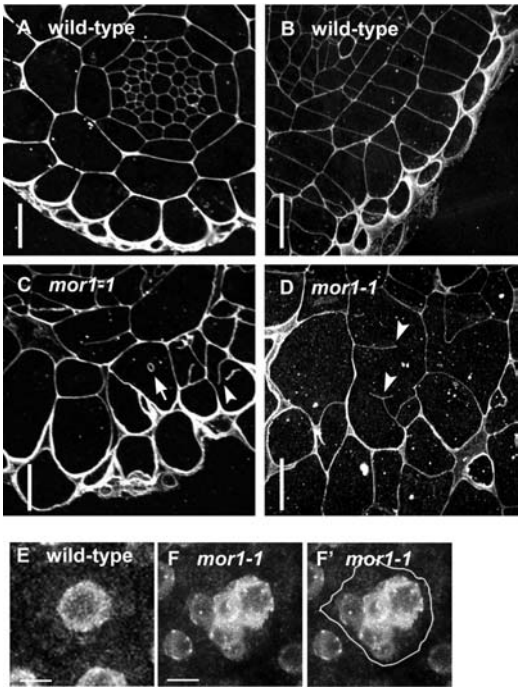

Figure 1. Cytokinesis defects are detected in the root tip of *mor1-1* at 31°C after 2 d for cell wall analysis and after 1 d for nucleus analysis. A to D, Cell walls of wild type (A and B) and *mor1-1* (C and D) are revealed by immunolabeling transverse (A and C) and longitudinal (B and D) sections with an antixyloglucan. In addition to obvious aberrant cell shapes, incomplete cross walls, cell wall inclusions, and wall stubs are indicated (arrows and arrowheads). Projections of confocal z-series. E and F, DAPI staining of whole mounted intact roots showing a single nucleus in wild type (E) and a cluster of nuclei in *mor1-1* (F and F′). The cell periphery is outlined in F′. Projections of confocal z-series. Bars = 20 μm (A–D) and 5 μm (E and F).

express the green fluorescent protein (GFP)-microtubule-binding domain (MBD) of MAP4 (Granger and Cyr, 2001a). Plants were grown in culture chambers on a temperature-controlled stage, enabling individual cells in the division zone of roots to be observed for several hours. This demonstrated conclusively that mitosis and cytokinesis were significantly slower in *mor1-1*. As shown in Figure 3, spindles and phragmoplasts persisted longer in *mor1-1* (averages of 25.3 and 38.2 min, respectively) than in wild type (13.9 and 23.3 min, respectively). Interestingly, we observed that neighboring cells, both within cell files and in adjacent files, tend to enter mitosis and complete cytokinesis together in both wild-type and *mor1-1* plants. This indicates that the signals triggering and regulating cell division may extend beyond the confines of single cells.

mor1-1 PPBs Are Frequently Absent and Spindles and Phragmoplasts Are Disrupted in Vivo

By carefully analyzing time-lapse sequences of dividing cells, we determined that approximately one-half of the *mor1-1* cells (15 of 35 observed) did not form PPBs prior to spindle formation. Images were recorded at least every 5 min so that preceding images could subsequently be analyzed whenever a spindle was observed. In contrast, all wild-type cells monitored through cell division developed prominent PPBs before proceeding through mitosis. The structure of microtubule arrays in living, dividing *mor1-1* cells also differed from that in wild type (Supplemental Movies 1 and 2; Fig. 3, C and D). As shown in Figure 3D (0 min), when PPBs were detected in *mor1-1* cells, they were less extensively developed in comparison with wild-type PPBs (Fig. 3C [0 min]). All *mor1-1* spindles were very disorganized at first (Fig. 3D [9 min]) and took much longer to organize chromosomes into metaphase configurations. They also appeared shorter and approximately one-half (16 of 35 observed) were misaligned compared to wild type (*mor1-1*, Fig. 3D [21 min]; wild type, Fig. 3C [6 min]). Despite this, cells consistently progressed to telophase, as judged by eventual spindle degradation and phragmoplast formation. Phragmoplasts were also of abnormal appearance in *mor1-1* (Fig. 3D [27–60 min]) compared to wild type (Fig. 3C [18–27 min]). Almost one-half of the phragmoplasts observed in *mor1-1* cells (18 of 39) were misoriented and, in some cases, formed discontinuous arrays, which would likely be deleterious for completion of cytokinesis. As illustrated in Figure 3D, for example, the phragmoplast is oblique, in contrast to the plane of the PPB, which, in this case, is at right angles to the cell long axis. Misoriented phragmoplasts were not observed in the wild type.

Immunofluorescence Analysis Shows That Microtubule Arrays Involved in Cell Division Are Aberrant

To investigate microtubule organization in dividing cells in better detail, we used immunofluorescence microscopy on material that had been incubated for 24 h at 31°C prior to fixation. Cells were separated from one another by gentle squashing after partial digestion of cell walls. As shown in Figure 4, all microtubule structures, including PPBs, spindles, and phragmoplasts, showed a range of disorganization in *mor1-1*. PPBs in *mor1-1* (Fig. 4B) were partially split instead of

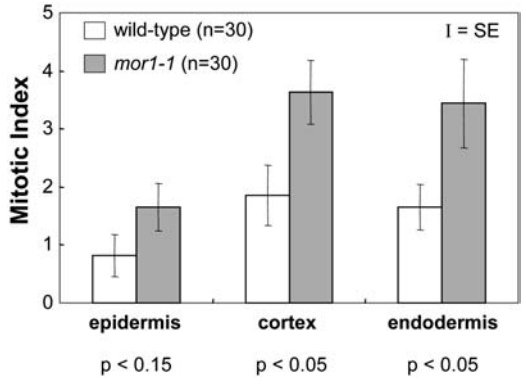

Figure 2. Higher mitotic indices in the *mor1-1* mutant suggest MOR1 is involved in cell division. The proportion of cells in mitosis is increased in *mor1-1* after 24 h at 31°C, suggesting that either mitosis is more frequent in the mutant or that mitotic progression is impaired.

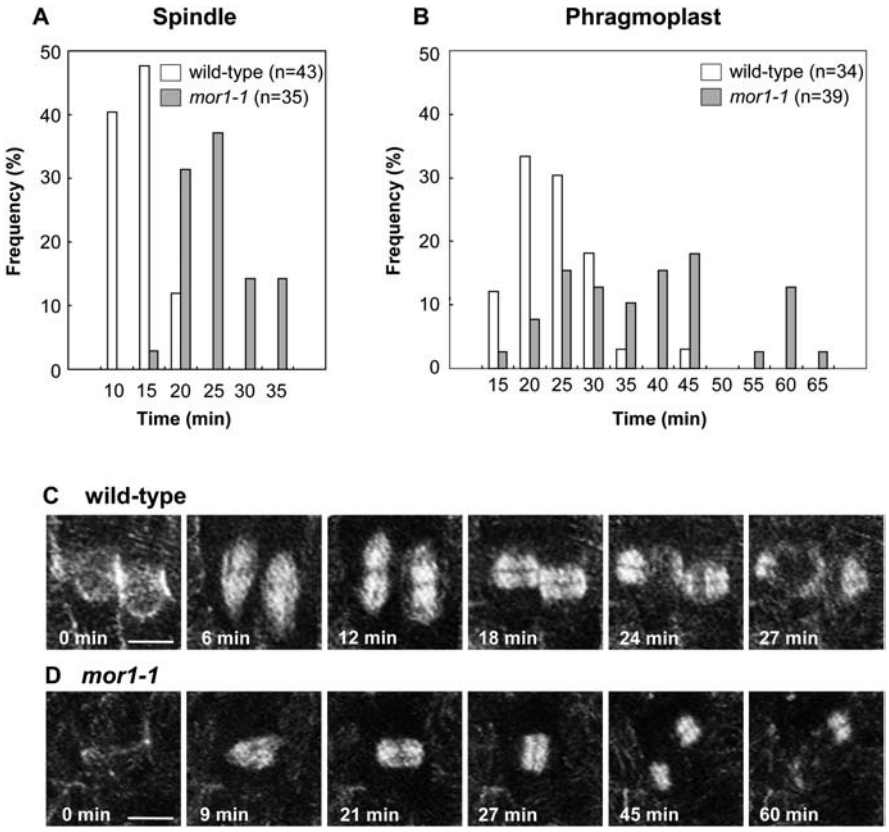

Figure 3. Analysis of microtubules in living cells using GFP-MBD fusion protein reveals that cell division takes longer and microtubule organization is aberrant in *mor1-1* at the restrictive temperature. A and B, Frequency distribution histograms show the ranges of time that individual spindles (A) and phragmoplasts (B) persist in wild-type (white bars) and *mor1-1* (gray bars) cells. C and D, Progression of mitosis and cytokinesis shown in a series of images from live root epidermal cells stably expressing the GFP-MBD fusion protein. In wild type, two adjacent cells show nearly synchronous progression of microtubule rearrangement during cell division (C). In *mor1-1* roots (D), a poorly developed PPB (0 min) is followed by a spindle, whose long axis is across the cell (9 and 21 min). A phragmoplast appears at 27 min, but eventually the microtubules show discontinuity (45 min). Like the spindle, the phragmoplast is not arranged in the orientation predicted by the PPB. Bars = 5 μm.

forming the continuous ring-like structures typical of wild type (Fig. 4A). Some spindles were severely disorganized, with misaligned short microtubules, resulting in some instances in complete disorganization of chromosomal arrangement (Fig. 4D). Other spindles had short microtubules but normally arranged chromosomes (Fig. 4E), whereas in other instances spindles were fragmented so that one or more pairs of chromosomes was separated from the others (Fig. 4F). Phragmoplasts were typically crooked and fragmented (Fig. 4H). These results confirm that the MOR1 protein has an important role in organizing not only cortical microtubules but also the microtubule arrays involved in cell division.

We carried out structural analysis of PPBs in *mor1-1* and wild-type cells (Fig. 4I). Taking into account the live cell analysis in which one-half of the dividing *mor1-1* cells failed to form PPBs, the true extent of PPB disorganization is underestimated in this analysis. Nevertheless, compared to wild-type cells, in which 96% of PPBs formed ring-like structures encircling the cell at the position of the nucleus, 80% of *mor1-1* PPBs were arranged this way (Fig. 4I). Wild type and *mor1-1* had the same proportion of acentric PPBs (3%), which are considered normal (Granger and Cyr, 2001b). However, *mor1-1* had an increased incidence of crooked PPBs (wild type, 1%; *mor1-1*, 7%). Six percent of *mor1-1* PPBs were discontinuous and 4% were branched, whereas aberrant PPBs were not observed in wild-type cells. In total, 17% of PPBs, when detected in *mor1-1*, were considered to be aberrant.

Phragmoplast organization was similarly analyzed (Fig. 4J). Wild-type phragmoplasts were observed in three typical configurations. Early on they were barrel shaped and, at later stages, formed double ring-like structures that were either continuous or discontinuous, the latter occurring when phragmoplasts reached the parent cell wall. In *mor1-1*, only 41% of phragmoplasts were deemed similar in appearance to wild-type phragmoplasts, whereas the remainder were considered aberrant. Approximately 40% of *mor1-1* phragmoplasts were crooked, compared to only 1% of wild-type phragmoplasts, and 9% of *mor1-1* phragmoplasts were severely fragmented. Other aberrant configurations accounted for another 10% of *mor1-1* phragmoplasts. To investigate whether the aberrant phragmoplasts led to defective cell plate formation, we examined callose accumulation in cells fixed during telophase. Callose, a major polysaccharide component of cell plates, accumulated at apparently normal levels in both wild type (Fig. 4K) and *mor1-1* (Fig. 4L). Callose in *mor1-1*, however, was often distributed in crooked, misoriented patterns, unlike the straight lines parallel to the parental cell cross walls in wild type.

Spindle and Phragmoplast Lengths Are Reduced in *mor1-1*

Typical *mor1-1* spindles were very short and not as focused as in wild type (Fig. 4, C–F). To compare spindle microtubule lengths, we measured metaphase

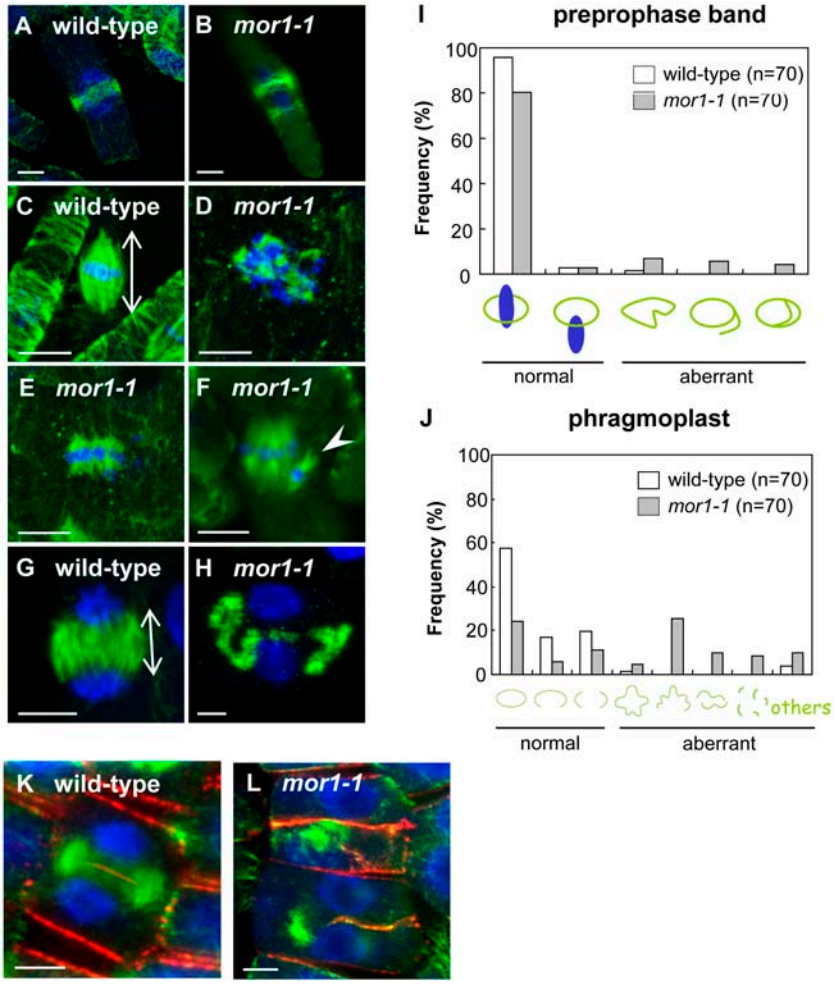

Figure 4. Immunofluorescence comparison of microtubule arrangement in root-tip cells of wild type and *mor1-1* after culture at 31°C for 24 h, and downstream consequences of defective mitosis and cytokinesis in *mor1-1*. A to H, Representative confocal images show antitubulin (green) and DAPI-stained nuclei and chromosomes (blue). Bars = 5 μm. A, Wild-type PPB. Projection of confocal z-series. B, *mor1-1* split PPB. Single optical confocal section. C, Wild-type spindle. Projection of confocal z-series. The double-headed arrow indicates how spindle length was measured (Fig. 5A). D to F, *mor1-1* spindles. Projections of confocal z-series (D and E) and a single optical confocal section (F). Arrowhead indicates uncoupled spindle component and associated chromosomes. G, Wild-type phragmoplast. Single optical confocal section. The double-headed arrow indicates how phragmoplast length was measured (Fig. 5B). H, *mor1-1* phragmoplast. Projection of confocal z-series. I and J, Quantitative analysis of PPB (I) and phragmoplast (J) arrangement in wild-type (white bars) and *mor1-1* (shaded bars) root-tip cells. Frequency distribution histograms are shown for each structural category, which are indicated in line drawings depicting normal and aberrant microtubule patterns with blue solid circles depicting nuclei. K and L, Immunolabeling with anticallose (red), antitubulin (green), and DAPI staining of DNA (blue) reveals a normal pattern of cell plate formation in wild-type (K) and crooked, misoriented cell plate in *mor1-1* (L). Single confocal optical sections. Bars = 5 μm.

and anaphase spindles in wild-type and *mor1-1* root-tip cells after 24 h at the restrictive temperature (Fig. 5A). The *mor1-1* spindles, with a mean length of 3.82 ± 0.93 (SD) μm, were significantly shorter than wild-type spindles ($P < 0.01$), which had a mean length of 8.82 ± 1.59 (SD) μm. Metaphase and anaphase spindle lengths were combined for these calculations because in *mor1-1* it was often difficult to distinguish metaphase and anaphase spindles due to the aberrant chromosomal arrangements. Metaphase and anaphase spindle lengths differed significantly in wild-type cells (Supplemental Fig. 1), but we found that spindles in *mor1-1* were significantly shorter than the metaphase spindles of wild type ($P < 0.01$). We considered the possibility that cell length regulates spindle size. In *mor1-1*, it was not possible to accurately measure cell length because of the crooked cross walls, but in wild-type cells we found no correlation between spindle and cell length (Supplemental Fig. 2). The reduction in spindle length in *mor1-1* mutants can therefore be attributed to the specific defect in the mutant protein.

Consistent with shorter spindles and disorganized cortical microtubules (Whittington et al., 2001), we found that phragmoplast arrays were shorter in *mor1-1* (Fig. 5B). We limited phragmoplast measurements to epidermal cells from roots grown for only 2 h at the restrictive temperature. This short time at the restrictive temperature produced wild-type and *mor1-1* epidermal cells of similar diameter and volume. This strategy allowed us to avoid measuring phragmoplasts in radially swollen cells of *mor1-1*, in which an obligate increase in phragmoplast diameter may dilute the tubulin pool and thereby reduce the length of microtubules. Phragmoplast length was measured as the combined length of microtubules in both halves of the phragmoplast array plus the phragmoplast clear zone (Fig. 4G, double-headed arrow). Preliminary analysis detected no significant difference in the length of early and late stage phragmoplasts in wild-type cells (Supplemental Fig. 3), so mean phragmoplast length was calculated from all phragmoplasts measured in both *mor1-1* and wild type. The mean phragmoplast length in *mor1-1* of 3.87 ± 0.45 (SD) μm was significantly less than the wild-type mean of 5.15 ± 0.51 (SD) μm ($P < 0.01$). These data indicate that MOR1 is important for maintaining the length of microtubules in phragmoplasts.

Of particular significance, all *mor1-1* phragmoplasts observed in the larger epidermal cells after this shift to

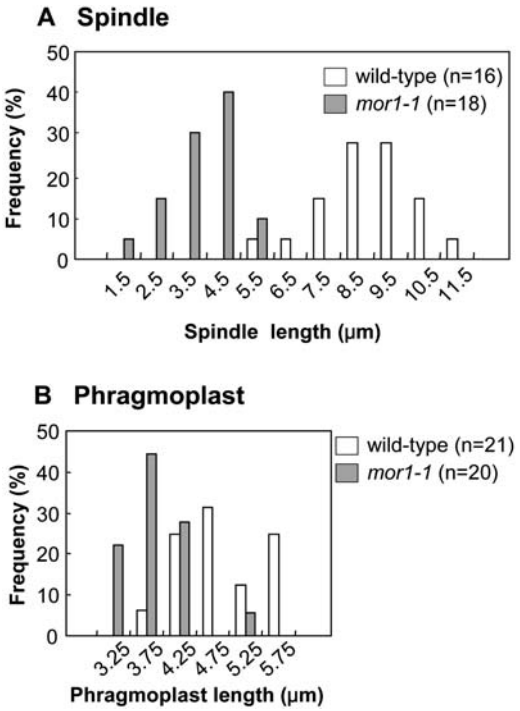

Figure 5. Immunolabeled spindles and phragmoplasts are significantly shorter ($P < 0.01$) in *mor1-1* at 31°C. Frequency distribution histograms compare wild type (white bars) and *mor1-1* mutants (gray bars), after culturing at 31°C for 24 h (spindle) and 2 h (phragmoplast). At least 20 spindles and 16 phragmoplasts were measured for each treatment, using image data collected from a confocal microscope. A, Spindle lengths, defined as the maximum distance from pole to pole, are significantly shorter in *mor1-1*. B, Phragmoplast length, defined as the greatest distance from one side of the phragmoplast array to the other, is almost consistently lower in *mor1-1*.

the restrictive temperature formed discontinuous, crooked structures and did not form the continuous ring-like configurations typical of wild-type phragmoplasts. This is in contrast to the 60% of cells sampled from all tissues with phragmoplast disruption after 24 h at the restrictive temperature. This finding suggests that controlling phragmoplast structure is a greater challenge in larger cells.

MOR1 Associates with Microtubules throughout the Cell Cycle, and This Association Is Not Lost in *mor1-1* at the Restrictive Temperature

We raised a polyclonal antiserum against residues 235 to 249 of MOR1 (hereafter anti-MOR1). Tubulin and MOR1 double labeling in wild-type cells showed that MOR1 is closely associated with cortical microtubules during interphase, and with PPBs, spindles, and phragmoplasts during cell division (Fig. 6, A–E). In contrast to a previous study using an antiserum raised against a MOR1 C-terminal polypeptide, which reported the MOR1 protein at the midzone of the phragmoplast and spindle (Twell et al., 2002), our antiserum recognized epitopes along the full length of microtubules in all arrays. As a second experimental proof that our antiserum reported an accurate distribution of MOR1 protein, we tested a polyclonal antiserum raised against an N-terminal epitope of the Xenopus homolog of MOR1, XMAP215 (Tournebize et al., 2000). This antibody gave similar full-length microtubule labeling as our antiserum (Supplemental Fig. 4, A–C) and did not label the phragmoplast midzone (Supplemental Fig. 4C). We found, however, that the XMAP215 antiserum also cross-reacted with an unknown epitope apparently distributed to the prominent dilated cisternae of the endoplasmic reticulum, making it unsuitable for detailed image analysis (Supplemental Fig. 4, B–F). Labeling of endoplasmic reticulum-dilated cisternae was not observed with $MOR1_{pep235\text{-}249}$ antiserum.

After 24 h at the restrictive temperature, there was no apparent reduction in MOR1 association with microtubules in either wild type (Fig. 6, A–E) or *mor1-1* (Fig. 6, F–J). Anti-XMAP215 also strongly labeled cortical microtubules that were disorganized after 4 h at the restrictive temperature (Supplemental Fig. 4, G and H). These results indicate that rapid disorganization of microtubules at the *mor1-1* restrictive temperature is caused neither by reduction in the amount of MOR1 present nor by the dissociation of the mutant form of the protein from microtubules.

Using immunofluorescence and immunoblotting analysis, we tested the specificity of the anti-MOR1 serum by preabsorbing with the antigen peptide (residues 235–249) to block MOR1-specific binding sites. Preabsorption completely removed all microtubule-specific labeling and also greatly reduced cytoplasmic fluorescence (Fig. 7, A and B), demonstrating that the majority of labeling and the microtubule colocalization, in particular, is MOR1 specific. Immunoblotting with anti-MOR1 identified a high-molecular mass band close to the MOR1 predicted molecular mass of 217 kD (Fig. 7C). Our antiserum, however, also consistently labeled several lower molecular mass bands. To determine whether these bands were proteolytic fragments of MOR1, we further resolved these bands on 10% mini gels and blotted with the same antigen peptide-preabsorbed anti-MOR1 serum used for immunofluorescence controls (Fig. 7A). This eliminated labeling of the approximately 30- and 60-kD bands, suggesting that these polypeptides are degradation products of MOR1 (Fig. 7D). Preabsorption did not, however, eliminate the labeling of two other approximately 50- and 20-kD bands, suggesting that these polypeptides are not recognized by the MOR1-specific immunoglobulin in the serum. Given the fact that the preabsorbed serum produced no microtubule-like labeling pattern (Fig. 7, A and B), it is unlikely that the approximately 50-kD band could be tubulin. Nevertheless, we confirmed that it was not tubulin by determining that the anti-MOR1 did not label purified tubulin on western blots (data not shown). Taken together, the immunofluorescence and immunoblotting data demonstrate that the microtubule labeling by the anti-MOR1 serum is specific to MOR1.

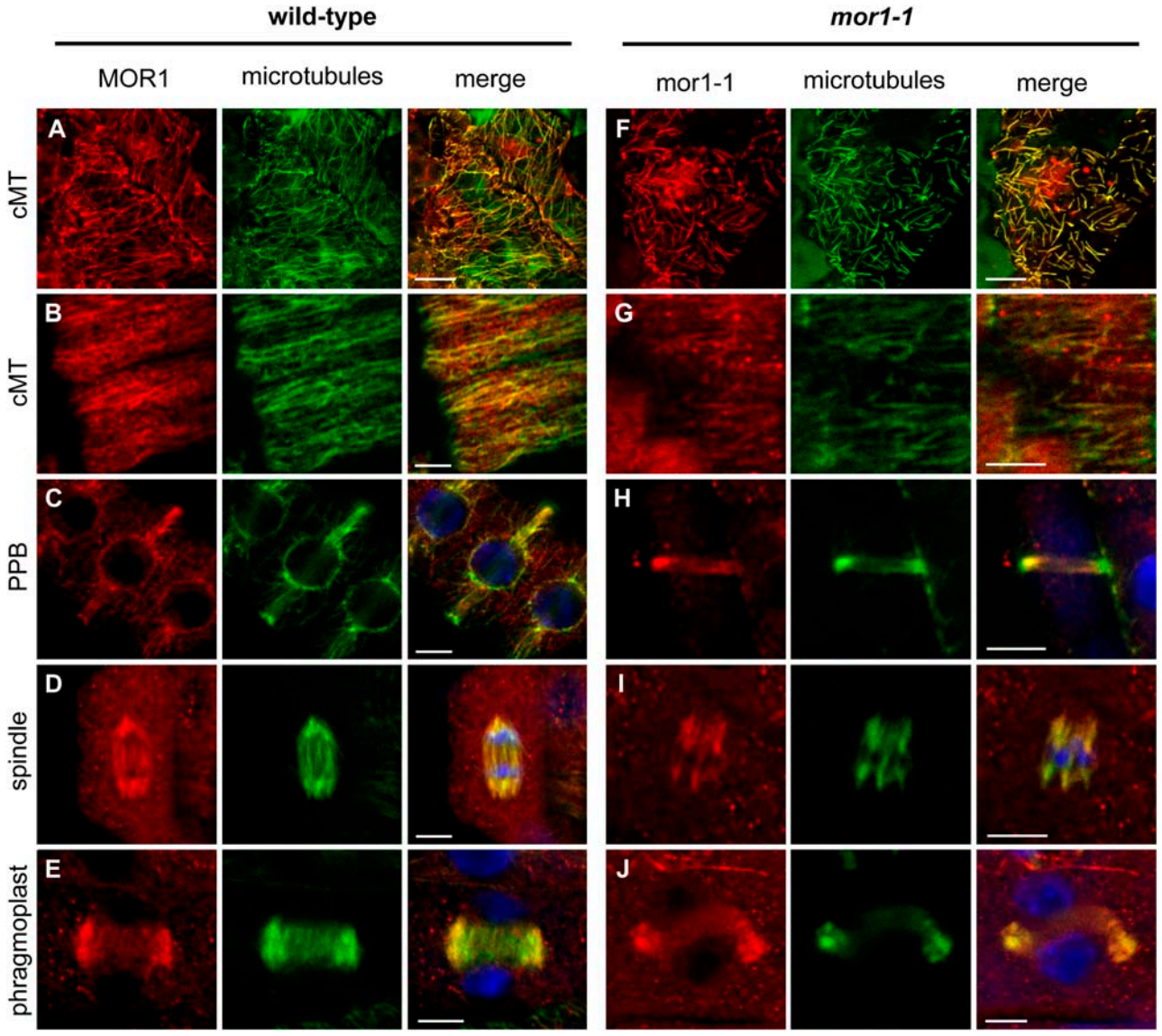

Figure 6. MOR1 protein associates along the entire length of microtubules throughout the cell cycle, and this association is not lost after 24 h at 31°C despite disruption of microtubule organization in *mor1-1*. Single optical sections from confocal z-series are used to demonstrate strict colocalization of anti-MOR1 (red) and antitubulin (green) in wild-type (A–E) and *mor1-1* (F–J). Yellow color in merged images reveals MOR1 and microtubule colocalization. Nuclei and chromosomes were DAPI stained (blue). A and F, Cortical microtubules in leaf epidermal cells. B to E and G to J, Root-tip cells showing interphase cortical microtubules (B and G), PPBs (C and H), spindles (D and I), and phragmoplasts (E and J). Bars = 10 μm (A and F) and 5 μm (B–E and G–J).

DISCUSSION

We demonstrate in this study that the MOR1 protein is situated along the entire length of microtubules at all stages of the cell cycle. We also show that the protein encoded by the *mor1-1* mutant allele remains associated with microtubules despite being unable to maintain microtubule organization at the restrictive temperature. This indicates that the *mor1-1* mutation does not prohibit the mutant protein mor1-1^{L174F} from binding to microtubules under restrictive conditions. Moreover, the *mor1-1* mutation can prevent formation of PPBs and, through its effects on microtubules, can dramatically affect the form and function of spindles and phragmoplasts. Loss of these functions slows the progression of mitosis and cytokinesis and sometimes prevents completion of cell division. These results extend previous functional analysis of the interphase array in the *mor1-1* mutant to provide novel insight into how MOR1 is involved in the formation and organization of PPBs, spindles, and phragmoplasts required for completion of cell division.

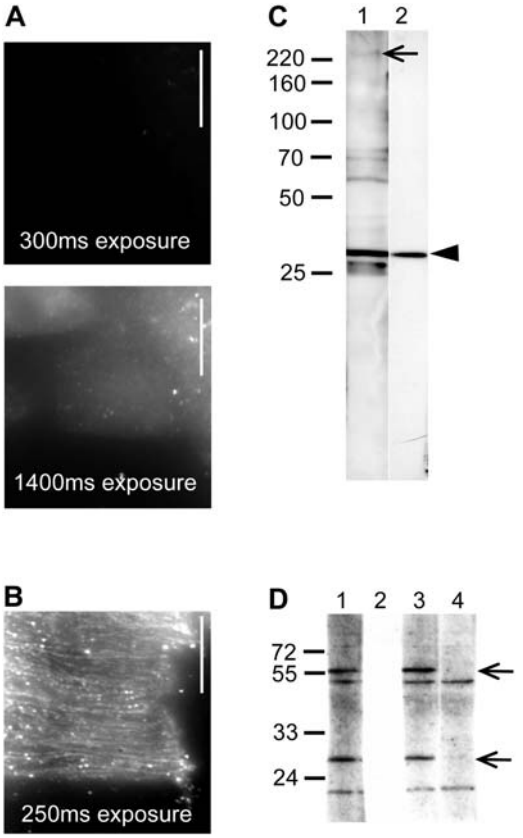

Figure 7. Immunofluorescence and immunoblotting analysis of wild-type Arabidopsis root tips and protein extracts with anti-MOR1 serum shows that the serum recognizes microtubules in a MOR1-specific manner. A, Overnight preabsorption of the polyclonal anti-MOR1 serum with the antigen peptide completely removed all microtubule-like fluorescent labeling in root-tip cells. Both images were taken from the same cells using different camera exposure times to demonstrate that even at the 1,400-ms exposure time required to detect fluorescence there is no microtubule-specific pattern. Bars = 5 μm. B, A control overnight incubation of the anti-MOR1 serum without the antigenic peptide demonstrates that the labeling of microtubules is not lost by this treatment. An exposure time of 250 ms was sufficient to detect microtubule labeling. Bar = 5 μm. C, Immunoblotting from a large gradient gel shows that anti-MOR1 (lane 1) recognizes a high-molecular mass band at approximately 220 kD (arrow) plus several low-molecular mass bands. Secondary antibody control (lane 2) demonstrates that the labeling of one of the low-molecular mass bands (arrowhead) is nonspecific. D, Immunoblotting the lower molecular mass bands resolved on a 10% mini gel demonstrates that two of these bands are likely to represent proteolytic degradation products of MOR1. Lane 1 shows four prominent bands. The secondary antibody control in this case included a blocking reagent that eliminated nonspecific binding (lane 2). Lanes 3 and 4 show the results of preabsorption with the antigen peptide. After overnight incubation of anti-MOR1 with no added peptide (lane 3), all four bands are still recognized. Anti-MOR1 preabsorbed overnight with the antigen peptide (lane 4), however, did not label bands of approximately 60 and approximately 30 kD (arrows). Two bands at approximately 50 and approximately 20 kD are still present, but, as indicated in A, these polypeptides are not microtubule localized.

MOR1 Distributes along the Entire Length of Microtubules throughout the Cell Cycle

Our immunolabeling demonstration that MOR1 associates along the entire length of microtubules is especially important in light of the wide variety of distribution patterns reported for members of the MAP215/Dis1 family. Depending on the method of labeling, cell type, or stage of the cell cycle, MAP215/Dis1 proteins have been observed at centrosomes and spindle pole bodies, distributed along the lengths of microtubules, or concentrated at microtubule plus ends (Gard et al., 2004). Our results suggest that MOR1 is less selective in its distribution along microtubules, a finding that may reflect the more dispersed nature of plant microtubule arrays, and the tendency of cortical microtubules to initiate new assembly at points along existing microtubules rather than at fixed organizing centers (Wasteneys, 2002; Van Damme et al., 2004b). Whereas some progress has been made in the use of GFP reporter fusions for examining the distribution of proteins involved in cytokinesis (Van Damme et al., 2004a), we have been unable, despite considerable ongoing effort, to produce suitable full-length fluorescent MOR1 reporter proteins to corroborate MOR1 distribution in live cells. The extreme size of the *MOR1* cDNA (6 kb) alone makes construct design and cloning extremely challenging, and, to our knowledge, fluorescent fusion constructs of plant proteins of this size have not been produced successfully.

In comparison to our antiserum, which was raised against a 15-amino-acid-long peptide from the N terminus of MOR1, two sera used in other studies have shown no strict colocalization along the full length of cellular microtubules. An antibody raised against a C-terminal fragment of MOR1 was reported to label spindle and phragmoplast midzones where microtubule plus ends are known to focus (Twell et al., 2002). In tobacco BY-2 cells, an antibody raised against purified MAP200, a tobacco homolog of MOR1, labeled in the vicinity of all microtubule arrays, rather than tightly overlapping with antitubulin signals, prompting Hamada et al. (2004) to suggest that MOR1/MAP200 shuttles cytoplasmic tubulin oligomers for polymerization at the plus ends of microtubules. Importantly, we found that an antibody raised against the N-terminal 560 amino acids of the MOR1 frog ortholog, XMAP215 (Tournebize et al., 2000), also labels the full length of microtubules in Arabidopsis cells, providing strong evidence that MOR1 is indeed distributed along the full length of microtubules in plant cells. Accessibility of the targeted epitope could explain the strikingly different labeling patterns produced by the two MOR1- and one MAP200-derived antibodies. Given the large size of these proteins, such variation in epitope affinity is not unexpected. Consistent with our peptide design strategy, the N-terminal epitope of MOR1 recognized by our antiserum appears to be freely exposed when MOR1 is bound to microtubules so that the antiserum will report a more

complete distribution. In contrast, the C-terminal epitope recognized by the Twell et al. (2002) antiserum may be less accessible to microtubule-bound MOR1, although it may be more exposed when MOR1 is associated with the plus ends of microtubules.

Our results suggest that MOR1 is an essential and integral part of functioning microtubules. We have shown that the *mor1-1* mutation in the N-terminal HEAT repeat does not abolish the ability of protein to bind microtubules. On the one hand, this observation supports the idea that the HEAT repeat affected by both the *mor1-1* and *mor1-2* mutations (Whittington et al., 2001) is involved in some function other than the binding of MOR1 to microtubules. In vitro binding assays indicate that the C-terminal region of MOR1 has microtubule-binding properties (Twell et al., 2002), although binding assays have not been performed on N-terminal regions of MOR1. Experiments have shown that the C-terminal region of the XMAP215 ortholog is critical for microtubule binding, while the N-terminal region has stabilizing properties that work antagonistically with destabilizing kinesins of the kin-1 class (Popov et al., 2001). Models have been put forward on how the *mor1-1* temperature-sensitive mutation in an N-terminal HEAT repeat may alter microtubule dynamics through a destabilizing kinesin (Hussey and Hawkins, 2001; Wasteneys, 2002). We have, however, carried out extensive investigations using the yeast two-hybrid assay to identify proteins that interact with the N-terminal region of MOR1 and have so far found no potential interactors (A.T. Whittington, P.R. Matthews, M.C. Rashbrooke, and G.O. Wasteneys, unpublished data). Similarly, there are no reports in the literature for the binding of the N-terminal region of the MOR1 orthologs to anything other than intact microtubules (Popov et al., 2001). Thus, the MOR1 N terminus may restrict access of destabilizing factors by competing for sites at the microtubule surface rather than through direct interactions while MOR1 remains attached to the microtubule (see model B in fig. 5 of Wasteneys, 2002).

Spindle Structure

The *mor1-1* phenotype of fragmented, short spindles that either do not focus or do not develop with multiple poles explains the higher mitotic indices recorded and the significant increase in the time required for *mor1-1* cells to complete mitosis at the restrictive temperature. Collectively, these spindle-associated defects could reflect a general consequence of a likely reduction in microtubule length, which alone might impede spindle structure and function. However, these observations also support the idea that MOR1 participates directly in overall spindle organization. Members of the MAP215/Dis1 family of proteins seem to be essential for spindle pole function and are found along with γ-tubulins and other proteins in centrosomes, which acquire spindle pole status during mitosis (Gard et al., 2004). Ch-TOG-depleted cells have aberrant chromosomal arrangements, which have been described as being in a prometaphase-like state (with no discernible metaphase plate) and as a metaphase plate with lagging chromosomes (Gergely et al., 2003). We observed these same two aberrant chromosomal arrangements in *mor1-1* at the restrictive temperature, suggesting that MOR1 located at the spindle pole regions, in addition to its distribution along the length of spindle microtubules, may be necessary for spindle organization. Plant cells lack mitotic centrosomes as well as tightly focused spindle poles, but γ-tubulins have been immunolocalized in spindle pole regions (Liu et al., 1994) and are likely to have important functions in microtubule assembly (Schmit, 2002). Therefore, the function of MOR1 in controlling nucleation of spindle microtubules, may, as with other MAP215 homologs, be through association with and regulation of γ-tubulin.

Phragmoplast Structure and Cytokinesis

The results of our study show that the *mor1-1* mutation disrupts phragmoplast organization in vegetative cells, leading to incomplete cell plate formation during telophase and production of multinucleate cells. We also observed cell wall stubs, wall inclusions, and incomplete and misoriented cell walls. These changes match those recently reported in the *mor1-1* mutant (Himmelspach et al., 2003a; Eleftheriou et al., 2005). According to Söllner et al. (2002), cytokinesis-defective mutants can be characterized by the presence of cell wall stubs in the division zone. By contrast, in mutants compromised in cell wall biosynthesis, incomplete cell walls will first be observed in more expanded cells (Söllner et al., 2002). After the shift to the restrictive temperature, aberrant walls first appear in *mor1-1* well within the cell division zone and not in the later stages of cell development (Whittington et al., 2001). Therefore, the *mor1-1*-induced defect is more likely to affect cell plate construction than wall biosynthesis. Importantly, these abnormalities resemble the aberrant cell wall formation observed in microspores from plants heterozygous for the *gem1* alleles of *MOR1* (Park and Twell, 2001; Twell et al., 2002). Some of the microspores inheriting the *gem1* alleles fail to produce a generative cell as a result of defective nuclear migration prior to pollen mitosis I and/or incomplete or aberrant (i.e. symmetrical) cell plate formation following pollen mitosis I (Park et al., 1998). Although the arrangement of phragmoplasts was not examined in the *gem1* microspores, it seems likely that their disruption would be a primary cause of the cell plate defects documented (Twell et al., 2002).

Twell et al. (2002) suggested MOR1/GEM plays an essential role in regulating the phragmoplast by stabilizing microtubule plus ends at the midline. This was based on their finding that a MOR1-specific antibody they raised was ''concentrated in the midline where oppositely orientated microtubules overlap in the spindles and phragmoplasts of isolated culture cells.''

Their conclusion, along with the report that the tobacco homolog of MOR1, TMBP200/MAP200, cross-links microtubules (Yasuhara et al., 2002), prompted the recent suggestion that GEM1/MOR1 may stabilize the growing plus ends of phragmoplast microtubules (Jürgens, 2005). Recent studies cast doubt on MOR1 playing a specific role in regulating the phragmoplast midzone. First, electron tomographic analysis has now demonstrated that oppositely oriented microtubules do not overlap at the phragmoplast midzone of somatic cells (Segui-Simarro et al., 2004; Austin et al., 2005). Second, the previous conclusion that TMBP200/MAP200 plays a role in cross-linking microtubules (Yasuhara et al., 2002) has been explained by the copurification of MAP65 protein in the MAP200 fraction (Hamada et al., 2004).

Our results also do not support the idea that the abnormal cell plates in the root tip of *mor1-1* mutants were formed by an irregular phragmoplast midzone. We found that the gap between microtubules at the midzone of the phragmoplast is similar in *mor1-1* and wild-type cells. Therefore, we suggest that the abnormal cell plates in *mor1-1* are produced by crooked, misoriented, and fragmented phragmoplasts. Some insights into the molecular mechanisms controlling cell plate formation may also come from other mutants affecting microtubule organization and cell plate formation, such as the kinesin mutant *hinkel* (Strompen et al., 2002) and the MAP65 mutant *pleiade* (*ple*; Müller et al., 2004). The *ple* mutant produces phragmoplasts that are longer than normal, with an increased clear zone between the two opposing microtubule arrays and increased microtubule lengths, resulting in incomplete cell plate formation and multinucleate cells. The general arrangement of *ple* phragmoplasts is not, however, altered (Müller et al., 2004). The different effects of *mor1-1* and *ple* mutants on phragmoplast formation underscore the very distinct functions of these two MAPs. The role of MAP65-3/PLE in microtubule cross-linking is supported by the substitution in the *ple-4* mutant of a conserved residue shown to be critical for microtubule-binding activity in the MAP65-1 paralog (Smertenko et al., 2004).

Cues for Positioning the Cell Plate

In comparison to spindles and phragmoplasts, PPB disorganization was less obvious in the *mor1-1* mutant. This relatively normal appearance, however, may reflect the difficulty in resolving details of this tightly packed array of cortical microtubules. Furthermore, in our live cell experiments, about one-half of the spindles observed formed in cells with no prior PPB formation, whereas in the wild type, all mitotic cells observed developed PPBs before spindles. The immunofluorescence data therefore underestimate the severity of the *mor1-1* mutant on PPB structure and also its PPB function. PPBs mark the site of attachment of the future cell plate (Mineyuki, 1999), although it remains unclear how this is achieved. Previous studies have shown that, although spindle orientation can affect subsequent phragmoplast position and orientation (Granger and Cyr, 2001b), considerable correction can take place as the cell plate is built, leading to fusion at the site originally marked by PPBs (Mineyuki and Gunning, 1990). In our live cell experiments, the early orientation of phragmoplasts in *mor1-1* cells consistently followed the preceding spindle orientation, but later stage phragmoplast positioning was highly variable and unpredictable. Even in the 50% or so of cells in which PPBs were documented, there was no clear relationship between PPB orientation and the eventual site of cell plate attachment. This could indicate that late phragmoplast misalignment is so severe that cues left by the PPB are irrelevant. In addition, it remains possible that the relatively normal-looking PPBs observed in *mor1-1* may not always function effectively in marking the cell plate attachment sites.

MOR1 Protein May Promote Long Microtubules

Our data support the idea that MAP215/Dis1 proteins promote relatively long microtubules. As with the previous discovery that cortical microtubules become short in the *mor1-1* mutant (Whittington et al., 2001), we found here that spindles and phragmoplasts were quantitatively shorter at the *mor1-1* restrictive temperature. The tobacco homolog of MOR1, TMBP200/MAP200, promotes increased microtubule length in vitro (Hamada et al., 2004). Taken together, these observations suggest that MOR1 has a general role throughout the cell cycle to control the length of microtubules and that microtubule length is critical for the organization and function of each array. Previous work supports the concept that the XMAP215 family members are primarily important for microtubule growth (Gard and Kirschner, 1987; Vasquez et al., 1994; Charrasse et al., 1998; Matthews et al., 1998; Tournebize et al., 2000; Lee et al., 2001; Whittington et al., 2001; Gräf et al., 2003).

In conclusion, the MOR1 protein plays an important role in organizing microtubule arrays at all stages of the cell cycle. The three homozygous-viable mutant alleles of *MOR1* described so far, including *mor1-1*, *mor1-2*, and *rid5*, all have single amino acid substitutions in the MOR1 conserved N-terminal TOG domain and generate conditional phenotypes (Whittington et al., 2001; Konishi and Sugiyama, 2003). While it remains possible that these three mutations confer novel functions, their common phenotypes provide useful insights into the normal function of the wild-type protein that cannot be obtained with lethal null alleles. In our current study, careful analysis of cells in the primary root division zone demonstrates that spindles, phragmoplasts, and PPBs are disorganized when seedlings are cultured at the high end of the restrictive temperature. In the original description of the *mor1-1* and *mor1-2* mutant phenotypes, it was noted that the first obvious morphological effect was left-handed twisting of organs (Whittington et al., 2001), which initiates in the elongation

zone (Sugimoto et al., 2003). This is followed after 24 h by an almost complete loss of growth anisotropy, resulting in severely swollen roots and other cylindrical organs. The gradual onset of this second-phase, more severe phenotype could reflect the cumulative effects of cell division anomalies, which will impair axialization (Wasteneys and Collings, 2004), a process that relies on auxin transport through well-defined tissue files. The defective microtubule patterns leading to the disruption of cell plate formation may therefore contribute to the loss of anisotropy and dwarfing that is characteristic of *mor1* and other cytokinesis-defective mutants. Analysis of the *rid5* allele suggested that the *rid5* mutation is detrimental to auxin signaling (Konishi and Sugiyama, 2003), indicating that the cross-talk between microtubule disruption and auxin signaling is an important area for future investigation.

MATERIALS AND METHODS

Plant Material and Growth Conditions

The Arabidopsis (*Arabidopsis thaliana*) *mor1-1* mutant (GenBank accession no. AF367246; Whittington et al., 2001), was backcrossed eight times to the parental Columbia ecotype. Control lines were segregated after the eighth backcross, and the F5 and F6 generations of both wild-type and *mor1-1* homozygous segregants were used in this study. Seedlings were cultured at 21°C as described (Himmelspach et al., 2003b). For temperature shift experiments, 5-d-old seedlings were transferred to a 31°C cabinet with similar light conditions to the 21°C cabinet.

Peptide-Specific Antibody Production

The MOR1 amino acid sequence was scanned for high surface probability regions using Peptidestructure on WebANGIS (www1.angis.org.au). A BLAST analysis was used to check that peptides designed were specific for MOR1. On this basis, five peptides representing different regions of the MOR1 protein sequence were synthesized and purified by HPLC (Biomolecular Resources Facility, Australian National University). Peptides were synthesized with an additional GC dipeptide at the C terminus and coupled to keyhole limpet hemocyanin (Sigma-Aldrich) using the heterobifunctional crosslinker *m*-maleimidobenzoyl-*N*-hydroxysuccinimide ester (Pierce Chemical). Coupled peptides were dialyzed exhaustively against phosphate-buffered saline (PBS; pH 7). New Zealand white rabbits were immunized using coupled peptide.

From these inoculations, only one serum, raised against the TRKIRSEQDKEPEAE peptide sequence found in the N-terminal region (amino acids 235–249) of MOR1, produced a promising labeling pattern. This serum, which we designate anti-MOR1$_{pep235-249}$, was affinity purified using HiTrap Protein G HP (Amersham Biosciences).

Immunoblotting

Seedlings were ground in liquid nitrogen and boiled for 3 min in sample buffer (final concentrations, 125 mM Tris, 0.8 mM EDTA, 20 mM dithiothreitol, 10% glycerol, 4% SDS, 0.001% bromphenol blue, pH 6.8). Extract was centrifuged at 15,000 rpm for 5 min and the supernatant was applied to a polyacrylamide gel for separation by electrophoresis. A 4% to 20% gradient gel was used to detect the full range of proteins, including the high-molecular mass bands, and a 10% gel was used to better resolve low-molecular mass bands recognized by components of the serum. Proteins were blotted onto a polyvinylidene difluoride membrane using a 12.5 mM Tris, 96 mM Gly, and 20% MeOH transfer buffer. Anti-MOR1 was diluted to 1/100 and 1/5,000 and was applied to blots from 4% to 20% gradient gels and 10% gels, respectively. For the anti-MOR1 peptide preabsorption assays, anti-MOR1 serum was incubated overnight with the original peptide antigen, peptide235-249 (anti-MOR1:peptide, 1 μL:1.2 mg), or without the peptide as a control, before applying to blots or use in immunofluorescence control experiments. Horseradish peroxidase-conjugated anti-rabbit IgG (Amersham Biosciences) was used as a secondary antibody. Blots from 4% to 20% gradient gels and 10% gels were developed using ECL Plus and Advance (Amersham Biosciences), respectively, according to the manufacturer's instructions.

Immunofluorescence Labeling of Root Tips

For immunolabeling intact roots, specimens were prepared as described (Collings and Wasteneys, 2005). For root-tip squashes, seedlings were fixed and processed according to Sugimoto et al. (2000) with the following modifications. The fixation buffer was preheated to the temperature at which seedlings were growing. Cell walls were digested for 30 min in an enzyme mixture composed of 0.1% (w/v) pectolyase Y-23 (Kikkoman), 0.1% (w/v) cellulysin (ICN), 1% bovine serum albumin, and 0.25 M sorbitol in PEM buffer (50 mM PIPES, 2 mM EGTA, 2 mM $MgSO_4$). Seedlings were washed with PEM plus Triton X-100 and the root tips (approximately 1 cm) were attached to microscope slides coated with 0.1% polyethyleneimine. Root tips were gently squashed in a solution of PEM buffer containing 0.25 M sorbitol by applying a glass coverslip and applying downward pressure while observing the root tip under a low-power dissection microscope. The coverslip was then removed by placing the slide on dry ice and then prying off the coverslip. Slides were incubated in PBS (130 mM NaCl, 5 mM Na_2HPO_4, 1.5 mM KH_2PO_4, pH 7.4) containing 1% Triton X-100 (1–3 h) to permeabilize membranes, and washed in PBS (10 min). To reduce autofluorescence and nonspecific antibody binding, samples were first incubated in 1 mg/mL $NaBH_4$ in PBS (two washes over 30 min), then washed in 50 mM Gly in PBS (30 min). After antibody labeling, 4′,6-diamidino-2-phenylindole (DAPI; Sigma-Aldrich) diluted in PBS (1 μg/mL) was applied for 10 min. Then samples were washed with PBS (two washes over 30 min). Root tips were mounted in Citifluor AF1 antifade agent.

Immunofluorescence of Anti-MOR1 Preabsorbed with the MOR1 Peptide235-249

Root-tip squashes were prepared from 6-d-old seedlings as described above. Anti-MOR1 (1/30) was incubated overnight with peptide235-249 (anti-MOR1:peptide, 1 μL:1.2 mg) or without the peptide as a control, before applying to root tips. As a secondary antibody, goat anti-rabbit Alexa Fluor 488 (1/200) was used (Molecular Probes).

Antibodies Used and Combinations for Double-Labeling Experiments

Primary antibodies included mouse anti-α-tubulin (clone B512 diluted 1/1,000; Sigma-Aldrich); mouse anti-β-tubulin (clone N357 diluted 1/100; Amersham); rabbit anti-soy tubulin (1/200; generously provided by Dr. Richard Cyr, Pennsylvania State University); mouse anti-β-1,3-glucan (callose; 1/50; Biosupplies); and rabbit anti-MOR1$_{pep235-249}$ (1/30). Secondary antibody conjugates and the dilutions at which they were used included fluorescein-isothiocyanate (FITC)-conjugated sheep anti-mouse IgG antibody, FITC-conjugated sheep anti-rabbit IgG, and Cy5-conjugated goat anti-mouse IgG (diluted 1/80, 1/50, and 1/200, respectively; Silenus/Chemicon).

For double labeling of microtubules and MOR1 protein, mouse anti-β-tubulin and rabbit anti-MOR1 primary antibodies were applied together, followed by the Cy5-conjugated goat anti-mouse IgG and FITC-conjugated sheep anti-rabbit IgG secondary antibody, respectively. For double labeling of tubulin and callose, rabbit anti-soy tubulin antibody and mouse anticallose primary antibodies were applied together followed by FITC-conjugated sheep anti-rabbit IgG and Cy5-conjugated goat anti-mouse IgG secondary antibodies.

Immunolabeling Leaf Cortical Microtubules and MOR1

Plants were grown for 11 d at 21°C followed by 31°C for 1 d. First leaves were excised from seedlings directly into fixative as for roots. Leaves were processed for immunofluorescence by freeze shattering as described (Wasteneys et al., 1997).

DAPI Staining for Chromosome and Nuclei in Intact Roots

Wild-type and *mor1-1* plants were grown for 5 d at 21°C followed by 31°C for 1 d. Plants were fixed and washed as described above. DNA was stained with DAPI (1 μg/mL) for 10 min. Roots were washed three times for 10 min and mounted in Citifluor. Mitotic indices were calculated as the percentage of mitotic figures in a set number of cell files from 15 different roots. Epidermal, cortical, and endodermal files of wild type and *mor1-1* were measured separately.

Immunofluorescence Microscopy

Fluorescence images were collected with a Leica TCS-SP2 confocal microscope equipped with a UV laser or with a Bio-Rad Radiance 2000 confocal microscope (Zeiss) equipped with a MaiTai sapphire laser (Spectra-Physics) or a Zeiss Axiovert 200M inverted microscope equipped with an AxioCamHR camera (Zeiss). The 488-nm line of an Ar laser and the 633-nm line of a HeNe laser were used for FITC and Cy5 excitation, respectively, with the Leica system, along with a 63× NA 1.2 water-immersion lens and 8-fold line averaging. For the Bio-Rad system, the 488-nm line of the Kr laser and the 647-nm line of a red diode were used for FITC/GFP excitation and Cy5 excitation, respectively, along with a 60× NA 1.4 oil-immersion lens and Kalman 2 averaging. For the Zeiss system, filter set number 46 was used for Alexa Fluor 488 excitation and emission, along with a 100× NA 1.3 oil-immersion lens. Images were processed with Leica confocal software to construct three-dimensional animations (ImageJ; http://rsb.info.nih.gov/ij) for measurements and creation of movies from time-lapse imaging, and Adobe Photoshop 7.0 to adjust contrast, to switch colors of images collected from the green to the red channel and from the red to the green channel for MOR1 and microtubule double-labeling analysis, and to overlay the colored images.

Spindle and Phragmoplast Measurements

Measurements of spindle lengths and cell size were made on roots kept for 24 h at 31°C that were processed using the root-squashing immunolabeling method to isolate cells so that metaphase and anaphase figures could be identified. Only spindles with an obvious axis were used for measurement, and spindles like the one shown in Figure 4D were not included. Measurements of phragmoplasts were recorded from epidermal cells kept for 2 h at 31°C. To ensure accurate measurements, any spindles and phragmoplasts oblique to the axis of the Z-scan were discarded. Analysis of PPB and phragmoplast arrangement was carried out by the root-tip squashing method, with plants kept for 24 h at 31°C prior to fixation.

Live Cell Imaging of GFP-MBD Plants

Wild-type and *mor1-1* plants expressing GFP-MBD under the control of the cauliflower mosaic virus Pro_{35S} (original seeds generously provided by Dr. Richard Cyr, Pennsylvania State University) were cultured as described above. Four- to 5-d-old seedlings were transferred to the coverslip bottoms of culture dishes (Electron Microscopy Sciences) and coated with the above-described medium without Suc and agar, and with 0.7% type VII agarose (Sigma-Aldrich) added. Culture dishes were sealed with surgical tape and placed in a growth chamber (21°C). The dishes were positioned 45° off-vertical so that roots would grow under the agarose and along the coverslip. After 1 d, culture dishes were transferred to 31°C. For live cell imaging of microtubules at 31°C, a heated stage, Bionomic controller BC-100 (20-20 Technology), was used. Images were collected with a Bio-Rad Radiance 2000 confocal microscope as described above for FITC, using Kalman 1 averaging. Z-series images were collected every 5 min for general measurements and every 3 min for Figure 3 and Supplemental Movies 1 and 2 for up to 3 h. Image data were collected from individual samples that were at the restrictive temperature for more than 2, but less than 8, h. Orienting cells in horizontal positions appeared to generate a temporary reduction in the incidence of cell division between 2 to 4 h in the wild-type roots, but, interestingly, we did not encounter this problem in *mor1-1*. We suspect that the temporary reduction in the incidence of cell division may be generated because continued rapid elongation of the wild-type root tip at high temperature generates a more efficient bending response when roots are placed in a horizontal position for viewing on the microscope stage. Contact of the wild-type root tip with the coverslip may generate a touch signal that temporarily reduces cell division. Cell division resumed after 4 to 7 h, so image data were collected during this period.

Immunofluorescence Labeling of Xyloglucan in Root-Tip Cells

Seedlings grown for 5 d at 21°C followed by 2 d at 31°C were fixed by vacuum infiltration in 2.5% glutaraldehyde in 0.1 M cacodylate buffer for 90 min. After a 10-min wash in buffer, seedlings were postfixed in 1% OsO_4 in distilled water followed by distilled water rinses (three times for 15 min). Roots were dehydrated with ethanol and subsequently infiltrated in LR White. Roots were transferred into gelatin or BEEM polyethylene capsules filled with fresh LR White and cured at 60°C for 24 h. One-micrometer-thick sections from root tips embedded in LR White were cut using a Reichert-Jung Ultracut E ultramicrotome (Leica) and transferred onto microscope slides coated with 0.1% polyethyleneimine. Sections were dried onto the slides on a slide warmer (50°C for at least 30 min). Sections were incubated in 50 mM Gly/PBS (15 min) followed by 4 h in blocking buffer (1% [w/v] BSA and 2% fish gelatin in PBS). Sections were then incubated for 2 h at room temperature or at 4°C overnight in primary polyclonal antixyloglucan (kindly provided by Dr. A. Staehelin, University of Colorado) diluted 1/10 in blocking buffer. After rinses in PBS (three times for 15 min), specimens were incubated in sheep anti-rabbit IgG-FITC (diluted 1/20; Silenus/Chemicon) for 6 h at room temperature and subsequently washed in PBS (three times for 15 min). Sections were mounted in Citifluor imaged with the Leica confocal microscope as described above.

ACKNOWLEDGMENTS

We thank Lacey Samuels (Botany, University of British Columbia) for helpful comments on this manuscript and Richard Cyr (Penn State University) for GFP-MBD seed stocks and anti-soy tubulin, Andrew Staehelin (University of Colorado, Boulder) for antixyloglucan, and Andrei Popov (European Molecular Biology Laboratories, Heidelberg) for anti-XMAP215. We also thank Hannie Van der Honing (Botany, University of British Columbia) for help in designing the live cell imaging methods; Jan Elliot (Australian National University), Frank Sek (Australian National University), and Tony Arioli (Bayer Crop Science) for technical advice; and the Australian National University electron microscopy unit and the University of British Columbia bioimaging facility for technical support and advice.

Received August 17, 2005; revised November 18, 2005; accepted November 22, 2005; published December 23, 2005.

LITERATURE CITED

Austin JR II, Segui-Simarro JM, Staehelin LA (2005) Quantitative analysis of changes in spatial distribution and plus-end geometry of microtubules involved in plant-cell cytokinesis. J Cell Sci **118:** 3895–3903

Charrasse S, Schroeder M, Gauthier-Rouviere C, Ango F, Cassimeris L, Gard DL, Larroque C (1998) The TOGp protein is a new human microtubule-associated protein homologous to the *Xenopus* XMAP215. J Cell Sci **111:** 1371–1383

Collings DA, Wasteneys GO (2005) Actin microfilament and microtubule distribution patterns in the expanding root of *Arabidopsis thaliana*. Can J Bot **83:** 579–590

Eleftheriou EP, Baskin TI, Hepler PK (2005) Aberrant cell plate formation in the Arabidopsis thaliana *microtubule organization 1* mutant. Plant Cell Physiol **46:** 671–675

Gard DL, Becker BE, Romney SJ (2004) MAPping the eukaryotic tree of life: structure, function, and evolution of the MAP215/Dis1 family of microtubule-associated proteins. Int Rev Cytol **239:** 179–272

Gard DL, Kirschner MW (1987) A microtubule-associated protein from Xenopus eggs that specifically promotes assembly at the plus-end. J Cell Biol **105:** 2203–2215

Gergely F, Draviam VM, Raff JW (2003) The ch-TOG/XMAP215 protein is essential for spindle pole organization in human somatic cells. Genes Dev **17:** 336–341

Gräf R, Euteneuer U, Ho TH, Rehberg M (2003) Regulated expression of the centrosomal protein DdCP224 affects microtubule dynamics and

reveals mechanisms for the control of supernumerary centrosome number. Mol Biol Cell **14:** 4067–4074

Granger CL, Cyr RJ (2001a) Spatiotemporal relationships between growth and microtubule orientation as revealed in living root cells of Arabidopsis thaliana transformed with green-fluorescent-protein gene construct GFP-MBD. Protoplasma **216:** 201–214

Granger CL, Cyr RJ (2001b) Use of abnormal preprophase bands to decipher division plane determination. J Cell Sci **114:** 599–607

Hamada T, Igarashi H, Itoh TJ, Shimmen T, Sonobe S (2004) Characterization of a 200 kDa microtubule-associated protein of tobacco BY-2 cells, a member of the XMAP215/MOR1 family. Plant Cell Physiol **45:** 1233–1242

Himmelspach R, Williamson RE, Collings DA, Wasteneys GO (2003a) The cell wall in the microtubule organization mutant *mor1-1* (abstract no. 1274). *In* Plant Biology 2003, July 25–30, 2003, Honolulu. American Society of Plant Biologists, Rockville, MD, http://abstracts.aspb.org/pb2003/public/P71/1294.html

Himmelspach R, Williamson RE, Wasteneys GO (2003b) Cellulose microfibril alignment recovers from DCB-induced disruption despite microtubule disorganization. Plant J **36:** 565–575

Hussey PJ, Hawkins TJ (2001) Plant microtubule-associated proteins: the HEAT is off in temperature-sensitive mor1. Trends Plant Sci **6:** 389–392

Jürgens G (2005) Cytokinesis in higher plants. Annu Rev Plant Biol **56:** 281–299

Konishi M, Sugiyama M (2003) Genetic analysis of adventitious root formation with a novel series of temperature-sensitive mutants of *Arabidopsis thaliana*. Development **130:** 5637–5647

Lee MJ, Gergely F, Jeffers K, Peak-Chew SY, Raff JW (2001) Msps/XMAP215 interacts with the centrosomal protein D-TACC to regulate microtubule behaviour. Nat Cell Biol **3:** 643–649

Liu B, Joshi HC, Wilson TJ, Silflow CD, Palevitz BA, Snustad DP (1994) γ-Tubulin in Arabidopsis—gene sequence, immunoblot, and immunofluorescence studies. Plant Cell **6:** 303–314

Matthews LR, Carter P, Thierry-Mieg D, Kemphues K (1998) ZYG-9, a *Caenorhabditis elegans* protein required for microtubule organization and function, is a component of meiotic and mitotic spindle poles. J Cell Biol **141:** 1159–1168

Menges M, Hennig L, Gruissem W, Murray JA (2002) Cell cycle-regulated gene expression in Arabidopsis. J Biol Chem **277:** 41987–42002

Mineyuki Y (1999) The preprophase band of microtubules: its function as a cytokinetic apparatus in higher plants. Int Rev Cytol **187:** 1–49

Mineyuki Y, Gunning BES (1990) A role for preprophase bands of microtubules in maturation of new cell-walls, and a general proposal on the function of preprophase band sites in cell-division in higher-plants. J Cell Sci **97:** 527–537

Müller S, Smertenko A, Wagner V, Heinrich M, Hussey PJ, Hauser MT (2004) The plant microtubule-associated protein AtMAP65-3/PLE is essential for cytokinetic phragmoplast function. Curr Biol **14:** 412–417

Park SK, Howden R, Twell D (1998) The *Arabidopsis thaliana* gametophytic mutation *gemini pollen1* disrupts microspore polarity, division asymmetry and pollen cell fate. Development **125:** 3789–3799

Park SK, Twell D (2001) Novel patterns of ectopic cell plate growth and lipid body distribution in the Arabidopsis *gemini pollen1* mutant. Plant Physiol **126:** 899–909

Popov AV, Pozniakovsky A, Arnal I, Antony C, Ashford AJ, Kinoshita K, Tournebize R, Hyman AA, Karsenti E (2001) XMAP215 regulates microtubule dynamics through two distinct domains. EMBO J **20:** 397–410

Schmit AC (2002) Acentrosomal microtubule nucleation in higher plants. Int Rev Cytol **220:** 257–289

Segui-Simarro JM, Austin JR II, White EA, Staehelin LA (2004) Electron tomographic analysis of somatic cell plate formation in meristematic cells of Arabidopsis preserved by high-pressure freezing. Plant Cell **16:** 836–856

Smertenko AP, Chang HY, Wagner V, Kaloriti D, Fenyk S, Sonobe S, Lloyd C, Hauser MT, Hussey PJ (2004) The Arabidopsis microtubule-associated protein AtMAP65-1: molecular analysis of its microtubule bundling activity. Plant Cell **16:** 2035–2047

Söllner R, Glässer G, Wanner G, Somerville CR, Jürgens G, Assaad FF (2002) Cytokinesis-defective mutants of Arabidopsis. Plant Physiol **129:** 678–690

Strompen G, El Kasmi F, Richter S, Lukowitz W, Assaad FF, Jürgens G, Mayer U (2002) The *Arabidopsis HINKEL* gene encodes a kinesin-related protein involved in cytokinesis and is expressed in a cell cycle-dependent manner. Curr Biol **12:** 153–158

Sugimoto K, Himmelspach R, Williamson RE, Wasteneys GO (2003) Mutation or drug-dependent microtubule disruption causes radial swelling without altering parallel cellulose microfibril deposition in Arabidopsis root cells. Plant Cell **15:** 1414–1429

Sugimoto K, Williamson RE, Wasteneys GO (2000) New techniques enable comparative analysis of microtubule orientation, wall texture, and growth rate in intact roots of Arabidopsis. Plant Physiol **124:** 1493–1506

Tournebize R, Popov A, Kinoshita K, Ashford AJ, Rybina S, Pozniakovsky A, Mayer TU, Walczak CE, Karsenti E, Hyman AA (2000) Control of microtubule dynamics by the antagonistic activities of XMAP215 and XKCM1 in Xenopus egg extracts. Nat Cell Biol **2:** 13–19

Twell D, Park SK, Hawkins TJ, Schubert D, Schmidt R, Smertenko A, Hussey PJ (2002) MOR1/GEM1 has an essential role in the plant-specific cytokinetic phragmoplast. Nat Cell Biol **4:** 711–714

Van Damme D, Bouget F-Y, Van Pouke K, Inzé D, Geelen D (2004a) Molecular dissection of plant cytokinesis and phragmoplast structure: a survey of GFP-tagged proteins. Plant J **40:** 386–398

Van Damme D, Van Poucke K, Boutant E, Ritzenthaler C, Inzé D, Geelen D (2004b) In vivo dynamics and differential microtubule-binding activities of MAP65 proteins. Plant Physiol **136:** 3956–3967

Vasquez RJ, Gard DL, Cassimeris L (1994) XMAP from *Xenopus* eggs promotes rapid plus end assembly of microtubules and rapid microtubule polymer turnover. J Cell Biol **127:** 985–993

Wasteneys GO (2002) Microtubule organization in the green kingdom: chaos or self-order? J Cell Sci **115:** 1345–1354

Wasteneys GO, Collings DA (2004) Expanding beyond the great divide: the cytoskeleton and axial growth. *In* PJ Hussey, ed, The Plant Cytoskeleton in Cell Differentiation and Development, Vol 10. Blackwell Scientific, Oxford, pp 83–115

Wasteneys GO, Willingale-Theune J, Menzel D (1997) Freeze shattering: a simple and effective method for permeabilizing higher plant cell walls. J Microsc **188:** 51–61

Whittington AT, Vugrek O, Wei KJ, Hasenbein NG, Sugimoto K, Rashbrooke MC, Wasteneys GO (2001) MOR1 is essential for organizing cortical microtubules in plants. Nature **411:** 610–613

Yasuhara H, Muraoka M, Shogaki H, Mori H, Sonobe S (2002) TMBP200, a microtubule bundling polypeptide isolated from telophase tobacco BY-2 cells is a MOR1 homologue. Plant Cell Physiol **43:** 595–603